

ACCRETION BY THE SECONDARY IN ETA CARINAE DURING THE SPECTROSCOPIC EVENT: I. FLOW PARAMETERS

Noam Soker

ABSTRACT

We examine the influence of the gravity of the companion (the secondary) to the massive primary star η Carinae on the winds blown by the primary and the secondary. The two winds collide with each other after passing through two respective shock waves, and escape the system while strongly emitting in the X-ray band. While during most of the 5.5 years orbital period, the companion's gravity has a negligible effect on the winds, we find that near periastron, the companion's gravity may significantly influence the flow and the companion might accrete from the primary's wind under certain circumstances. Near periastron passage, the collision region of the two winds may collapse onto the secondary star, a process that could substantially reduce the X-ray luminosity. We suggest that such an accretion process produces the long, almost flat, X-ray minimum in η Carinae.

Subject headings: accretion—binaries: close—circumstellar matter—stars: individual: η Carinae—stars: mass loss

1. INTRODUCTION

η Carinae is a very massive star that underwent a twenty years long eruption, termed the Great Eruption, about 160 years ago (Davidson & Humphreys 1997). A massive nebula, $\gtrsim 12M_{\odot}$ (Smith et al. 2003b), expelled during the Great Eruption, formed the Homunculus—an expanding bipolar nebula around η Car (Morse et al. 1998); A smaller bipolar nebula is

¹Department of Physics, Technion—Israel Institute of Technology, Haifa 32000 Israel; soker@physics.technion.ac.il

believed to have been created during the Lesser eruption of 1890 as well (Ishibashi et al. 2003). It is widely accepted now that η Carinae is a massive binary system with an orbital period of 5.54 yr (e.g., Daminieli 1996; Daminieli et al. 1997, 2000; Ishibashi et al. 1999; Corcoran et al. 2001a,b; 2004b; Pittard & Corcoran 2002; Duncan & White 2003; Fernandez Lajus et al. 2003; Smith et al. 2004; Whitelock et al. 2004; Verner et al. 2005). The more massive companion of the η Car binary system will be referred to here as the primary, while the companion, probably an O-type star, will be referred to as the secondary.

The binary nature of η Car is inferred from the periodicity of the so-called spectroscopic event—the fading of high excitation lines (e.g., Daminieli et al. 2000). Since the spectroscopic event might in principle result from a mass-shell ejection by the primary star (Zanella et al. 1984; Davidson et al. 1999; Smith et al. 2003a; Martin & Koppelman 2004), it is also called a shell ejection event. The main motivation to assume a shell ejection is in a single star model; in the binary model the shell ejection is not necessary, although it might occur (Soker 2005). The same periodicity is seen in many wave bands, from the IR (e.g., Whitelock et al. 2004), to the X-ray (Corcoran et al. 2001a; Corcoran 2005; Corcoran et al. 2004a,b). The period derived from the spectroscopic events is ~ 5.54 yr (2023 ± 3 days as given by the IR lightcurve of Whitelock et al. 2004), and is believed to represent the orbital period. The orbit is believed to have a very high eccentricity. For primary and secondary masses of $M_1 = 120M_\odot$ and $M_2 = 30M_\odot$, respectively, the semi major axis of the orbit is $a = 16.6$ AU (there is not yet agreement on all the binary parameters, e.g., Ishibashi et al. 1999; Daminieli et al. 2000; Corcoran et al. 2001a, 2004b; Hillier et al. 2001; Pittard & Corcoran 2002; Smith et al. 2004).

Less agreement exists concerning the role of the secondary in the shaping of the wind from the primary in η Car. Based on multi-color photometry van Genderen et al. (1994, 1995, 1999) proposed the presence of an accretion disk around a secondary star before the periodicity of the spectroscopic event was discovered (Daminieli 1996). Based on theoretical calculations Soker (2001b, 2003, 2004, 2005) argued that a single star cannot explain many of the properties of η Car, in particular that a single star cannot account for the bipolar shape of the Homunculus. Instead, those papers argued that the secondary accreted a large fraction of the mass that was expelled in the Great Eruption forming an accretion disk and two jets which shaped the wind of the primary into the bipolar Homunculus (Soker 2001b). Soker (2003, 2005) discusses the formation of an accretion disk in the present day binary system, in agreement with some of the suggestions made by van Genderen et al. (1994, 1995, 1999).

Soker (2005) discussed three basic accretion phases, two of which occur in the present day. Both stars blow winds, with the primary’s wind having a much larger mass loss rate

and a lower velocity. The winds collide, and at one location the momentum fluxes of the two winds exactly balance each other, forming a stagnation point. The stagnation point is located close to, but not exactly on, the line joining the centers of the two stars because of orbital motion. The shocked material of the primary star cools very fast (Pittard & Corcoran 2002; see eq. 1 in Soker 2003), namely, before the mass moves far from the stagnation point. The surrounding pressure then compresses the cooled post-shock gas to high densities. When blowing the wind, radiation pressure on the escaping gas overcomes gravitational attraction. However, this might not be the case with the dense gas near the stagnation point. Gravitational force on the dense and slowly moving (much below escape velocity) gas there might become large enough to accrete part of the mass back onto one of the stars. Whether accretion occurs at all, and if it does, which of the two stars accrete most of the gas depends on the accretion phase of η Car:

1. **The Great Eruption.** The mass loss rate by the primary was very high, and the stagnation point was within the secondary’s Bondi-Hoyle accretion radius. Along the entire orbit the secondary steadily accreted mass with high specific angular momentum. An accretion disk was formed and two jets (or a collimated fast wind—CFW) were launched (Soker 2001b). According to Soker (2001b) these jets shaped the two lobes which are now observed as the Homunculus.
2. **Apastron passages.** Soker (2003) proposed that during present apastron passages the primary itself can accrete $\sim 5\%$ of the mass lost over an entire orbit. This should not be confused with the accretion fraction of $\sim 50\%$ by the secondary during the 20 year span of the Great Eruption. The high specific angular momentum of the accreted gas implies the formation of an accretion disk around the primary. The primary star might blow a CFW.
3. **Periastron passages.** Near periastron passages, which occur near the spectroscopic events, short accretion episodes might occur, possibly leading to pulsed ejection of two jets by the secondary (Soker 2005). This accretion process was proposed but not studied by Soker (2005). The secondary might also ionize a non-negligible region in its surrounding neighborhood.

This paper presents further exploration of the nature of the wind interaction near periastron passage. In the next section we compare the typical time scales and length scales of several processes during the periastron passage. The reader interested only in the main points of the proposed model can skip section 2 and go directly to section 3, where we discuss how these may allow an accretion event onto the secondary star for several weeks near periastron passage. Our main results are summarized and discussed in section 4.

2. RELEVANT LENGTH AND TIME SCALES AT PERIASTRON

2.1. Length Scales

We calculate the distance of the stagnation point of the secondary’s wind taking into account the orbital motion; by orbital velocity we refer to the relative orbital velocity of the two stars. Following Usov (1992), we take the wind with the larger momentum flux, in our case the primary’s wind, to be plane parallel near the secondary star. Because of the orbital motion, the stagnation point of the secondary’s wind will be ahead of the line joining the centers of the two stars (Figure 1). The radial (along the line joining the two stars) component of the relative velocity between the secondary star and the primary’s wind is $v_1 - v_r$, where v_1 is the radial component of the primary’s wind speed and v_r the radial component of the orbital velocity; v_r is negative when the two stars approach each other. Because the stagnation point is very close to the secondary star, we assume that this is also the relative radial velocity of the stagnation point to the primary’s wind. The total relative speed between the stagnation point and the primary’s wind is

$$v_{\text{wind1}} = (v_\theta^2 + (v_1 - v_r)^2)^{1/2}, \quad (1)$$

where v_θ is the tangential component of the orbital velocity. We neglect any time delay between ejection of the wind by the primary and its collision with the secondary’s wind. This assumption is justified over most of the orbit, but not near periastron, where the orbital and primary’s wind speed are almost equal. However, the uncertainties because of this assumption are less problematic than the uncertainties caused by our ignorance on the exact velocity profile of the primary’s wind, i.e., its acceleration over a distance of ~ 3 AU, and a possible enhancement in the primary’s mass loss rate near periastron. At the stagnation point the ram pressures of the two winds are equal

$$\rho_1 v_{\text{wind1}}^2 = \rho_2 v_2^2, \quad (2)$$

where v_2 is the secondary’s wind speed, assumed to be much larger than all other flow velocities in the problem.

The respective wind densities are

$$\rho_i = \frac{\dot{M}_i}{4\pi D_i^2 v_i}, \quad i = 1, 2, \quad (3)$$

where D_i is the distance from the respective star to the stagnation point (Figure 1). Substituting the expressions for the winds’ densities in equation (2) gives

$$\frac{1}{D_1^2} \frac{v_{\text{wind1}}^2}{v_1^2} = \frac{\beta^2}{D_2^2}, \quad (4)$$

where

$$\beta \equiv \left(\frac{\dot{M}_2 v_2}{\dot{M}_1 v_1} \right)^{1/2}. \quad (5)$$

As we see β depends on the orbital separation because near periastron it is assumed that the primary’s wind does not yet reach its terminal speed.

Let ϕ be the angle measured from the secondary between the direction to the primary and that to the stagnation point (Figure 1). The following trigonometric relation holds $D_1^2 = D_2^2 + r^2 - 2rD_2 \cos \phi$, where r is the orbital separation, and $\cos \phi = (v_1 - v_r)/v_{\text{wind1}}$. Substituting for D_1 in equation (4) gives an equation which can be solved for D_2 ,

$$D_2 = \beta r \left\{ \left[\left(\frac{v_1 - v_r}{v_{\text{wind1}}} \right)^2 \beta^2 + \frac{v_{\text{wind1}}^2}{v_1^2} - \beta^2 \right]^{1/2} - \frac{v_1 - v_r}{v_{\text{wind1}}} \beta \right\} \left(\frac{v_{\text{wind1}}^2}{v_1^2} - \beta^2 \right)^{-1}. \quad (6)$$

Near periastron the gravitational influence of the secondary on the flow near the stagnation point should be considered. This effect on the undisturbed primary’s wind is characterized by the Bondi-Hoyle accretion radius

$$R_{\text{acc2}} = \frac{2GM_2}{v_{\text{wind1}}^2} = 0.2 \frac{M_2}{30M_\odot} \left(\frac{v_{\text{wind1}}}{500 \text{ km s}^{-1}} \right)^{-2} \text{ AU}. \quad (7)$$

The relative speed v_{wind1} is scaled for periastron passage, where $v_{\text{orb}} \simeq 400 \text{ km s}^{-1}$, $v_1 \sim 300 \text{ km s}^{-1}$, since the primary’s wind did not yet reach its terminal speed of $\sim 500 \text{ km s}^{-1}$. Martin et al. (2005), for example, take the primary’s wind speed to be $v_1 \simeq 500(r/3 \text{ AU}) \text{ km s}^{-1}$ for $r < 3 \text{ AU}$, and $v_1 \simeq 500 \text{ km s}^{-1}$ for $r \gtrsim 3 \text{ AU}$. When approaching periastron v_{wind1} will be larger than its value when leaving periastron. This results in a much larger accretion radius when leaving periastron, as described in the next section.

As in the classical Bondi-Hoyle-Lyttleton accretion flow, the density and velocity of the inflowing gas increase as the gas approaches the gravitating point mass. This increases the ram pressure of the primary’s wind, and according to equations (2) and (3) the stagnation point distance from the secondary changes as $D_2 \propto (\rho v^2)^{-1/2}$. Using the density (from Danby & Camm 1957) and the velocity (from energy conservation) along the symmetry axis in the upflow direction (ahead of the stagnation point), one finds the stagnation distance when the secondary’s gravity is considered

$$D_{g2} = 2 \left(1 + \frac{R_{\text{acc2}}}{D_2} \right)^{-1/4} \left[1 + \left(1 + \frac{R_{\text{acc2}}}{D_2} \right)^{1/2} \right]^{-1} D_2. \quad (8)$$

For the parameters used here, $R_{\text{acc2}}/D_2 \simeq 0.5$ near periastron, hence $D_{g2} \simeq 0.8D_2$ near periastron. Some of the quantities derived in this section are plotted on Figure 2.

2.2. Time scales

As shown by several authors (e.g., Pittard & Corcoran 2002; Soker 2003), at all orbital phases the cooling time of the shocked primary’s wind is much shorter than the flow time of the gas out of the shocked region. The post shocked primary’s wind in a large area near the stagnation point cools and is compressed by the ram pressure of the colliding winds. As shown by Soker (2005) cold and dense blobs of size $r_b \gtrsim 0.001D_2$ will be accreted by the secondary. One of the uncertainties in this study involves the exact velocity profile and terminal velocities of the two winds. In particular, the radiation from one star can influence the velocity profile of the wind from the other star before the winds collide (Gayley et al. 1997). In any case, we estimate these uncertainties to be minor. The secondary star radius is about an order of magnitude smaller than the distance to the stagnation point. Hence, it is already at its terminal velocity, assuming that the radiation pressure of the primary does not slow down much the secondary wind. This is justified by (i) the calculations of Pittard & Corcoran (2002) of the X-ray emission, that show the secondary wind to be shocked at $v_2 \sim 3000 \text{ km s}^{-1}$, with little variation in the shocked gas temperature over most of the orbit (Ishibashi et al. 1999), and (ii) by the location of the stagnation point far from the primary. For the primary wind we assume a simple velocity profile in section 2.3. Taking other reasonable wind properties for $\eta \text{ Car}$ from the literature will not change much the results of this paper.

In section 3 we propose that mass from the shocked primary wind is accreted for ~ 80 days near periastron passage. This phase begins with accretion of dense blobs. We now estimate the blobs’ properties following (2005). We consider a post-shock spherical blob of mass m_b , density ρ_b , and radius R_b , located at a distance r_2 from the secondary of mass M_2 . We make three assumptions. (i) Because of the short radiative cooling time mentioned above, the temperature of the blob is $T_b = 10^4 \text{ K}$, (ii) The blobs are in pressure equilibrium with the ram pressure of the secondary’s wind so that at any distance r_2 , $\rho_b k T_b / (\mu m_H) = \rho_2 v_2^2$, where μm_H is the mean mass per particle in the blob, and k is the Boltzmann’s constant. Using the assumed values of $\dot{M}_2 = 10^{-5} M_\odot \text{ yr}^{-1}$ and $v_2 = 3000 \text{ km s}^{-1}$ (see section 2.3) gives

$$\rho_b = 5 \times 10^{-11} \left(\frac{r_2}{1 \text{ AU}} \right)^{-2} \text{ g cm}^{-3}. \quad (9)$$

The mass in one blob is

$$m_b = 7 \times 10^{-10} \frac{\rho_b}{10^{-10} \text{ g cm}^{-3}} \left(\frac{R_b}{0.01 \text{ AU}} \right)^3 M_\odot. \quad (10)$$

(iii) The radiative pressure of the secondary plays a minor role. This comes from two reasons.

First, the ratio of the ram pressure of the secondary wind to the secondary radiation pressure is

$$\xi \equiv \frac{P_{2\text{rad}}}{P_{2\text{ram}}} \simeq \frac{L_2/c}{M_2 v_2} = 0.6 \left(\frac{L_2}{9 \times 10^5 L_\odot} \right), \quad (11)$$

where the secondary luminosity is scaled according to Verner et al. (2003). Namely, the radiation pressure adds to the secondary ram pressure, but not more than 60%. The second reason is that near the stagnation region, where it is determined whether accretion takes place, the radiation pressure by the primary acts in the opposite direction to that of the secondary. As can be seen from Figure 2, the distance of the stagnation region from the primary ($r - D_{g2}$) is ~ 3 times the distance to the secondary (D_{g2}). However, the primary luminosity is estimated to be ~ 10 times that of the secondary. Since the radiation pressure drops as $1/(\text{distance})^2$, we find that the radiation pressure of the primary, which pushes the gas toward the secondary, more than compensates for the secondary radiation pressure near the stagnation point. This holds as long as $L_1 \gtrsim 10L_2$. Considering radiation pressure by both stars will actually increase the effects studied in the present paper.

The condition for accretion, therefore, is that the gravitational force

$$f_g = \frac{GM_2 m_b}{r_2^2} \quad (12)$$

on a blob be larger than the force due to ram and radiation pressure of the secondary wind

$$f_{w2} = \rho_{w2} v_2^2 \pi R_b^2 (1 + \xi). \quad (13)$$

Substituting the typical physical values used here and equation (9) in the condition for accretion $f_g > f_{w2}$, gives the constraint on the size of the accreted blob

$$R_b > 0.004(1 + \xi) \left(\frac{r_2}{1 \text{ AU}} \right)^2 \text{ AU}. \quad (14)$$

This shows that even very small blobs can be accreted. Substituting values in the last equation, we find $R_b > 0.007 \text{ AU}$ for $r_2 = D_{g2} = 1 \text{ AU}$, when the orbital separation is $r \sim 4 \text{ AU}$ (accretion is not expected to start earlier than this time) According to the last equation closer to the secondary even smaller blobs can be accreted. By equations (14), and (10) with (9), the minimum mass allowed for accreted blobs goes as $m_b \propto r_2^4$. Namely, as a blob moves toward the secondary, even if it breaks to smaller blobs, these may still be accreted if they are not too small. The blobs near the stagnation point can be somewhat smaller than the constraint given by equation (14) because the radiation pressure of the primary pushes toward the secondary.

The last point should be emphasized. If the flow structure was such that the primary wind streams undisturbed toward the secondary star, to the point where the secondary

radiation pressure is larger than the primary radiation pressure $L_2/r_2^2 > L_1/(r - r_2)^2$, then the radiation pressure could have slowed down or could even expel the incoming primary wind; a process termed radiative braking (e.g., Gayley et al. 1997). However, the primary wind encounters a shock wave *before* radiative braking starts. Dense blobs are likely to form in this unstable interaction region. We conclude that the radiation pressure and ram pressure cannot prevent the accretion by the secondary of even small blobs.

As discussed in section 3, if the stagnation region collapses the maximum steady state accretion rate is $\dot{M}_{\text{acc}2} \sim 10^{-6} M_\odot \text{ yr}^{-1}$. When the stagnation region collapses before or near periastron, the accretion radius is smaller and the Bondi-Hoyle formula will give a lower accretion rate. However, if (as proposed in the next section) the entire stagnation region collapses, we can still crudely take an accretion rate of $\sim 10^{-6} M_\odot \text{ yr}^{-1}$. As shown below the accretion dynamical time scale is $\sim 0.01 \text{ yr}$. Using the typical blob mass from equation (10), we find that ~ 10 blobs exist during the collapse of the stagnation point region. These blobs when accreted onto the secondary *are assumed* to vigorously disturb the acceleration region of the secondary wind, such that practically the secondary wind ceases to exist. For the rest of the flat minimum phase, we assume that there is no wind collision and the accretion flow is that of the Bondi-Hoyle-Lyttleton type. That the accreted primary wind almost completely shuts down the secondary wind is a strong assumption of the present paper, and must be checked in future calculations of the acceleration zones of accreting O stars, and observations of $\eta \text{ car}$ during minimum.

The free fall time from the stagnation point to the secondary is

$$\tau_{\text{ff}2} = 1.05 \left(\frac{M_2}{30M_\odot} \right)^{-1/2} \left(\frac{D_{g2}}{0.2 \text{ AU}} \right)^{3/2} \text{ day}. \quad (15)$$

The outflow time from the stagnation point is somewhat longer than the flow of the undisturbed primary wind

$$\tau_{\text{flow}1} \gtrsim \tau_{\text{fl}} \equiv \frac{D_{g2}}{v_{\text{wind}1}} = 0.69 \frac{D_{g2}}{0.2 \text{ AU}} \left(\frac{v_{\text{wind}1}}{500 \text{ km s}^{-1}} \right)^{-1} \text{ day}. \quad (16)$$

The cooling time of the secondary's wind is longer than the flow time $\tau_{\text{flow}2}$; for $v_2 = 3000 \text{ km s}^{-1}$ $\tau_{\text{flow}2} > \tau_{f2} \equiv 0.1(D_{g2}/0.2 \text{ AU})$ days. However, near periastron when the stagnation distance D_{g2} becomes small, the cooling of gas very close to the stagnation point becomes non-negligible because very close to the stagnation point $\tau_{\text{flow}2} \gg \tau_{f2}$ (Usov 1991). The secondary's wind is shocked to a temperature of $\sim 10^8 \text{ K}$, where the cooling function dependence on temperature is $\Lambda = \Lambda_0 T^{0.4}$. The cooling time at constant pressure is $\tau_{\text{cool}2} = (5/2)nkT(n_e n_p \Lambda)^{-1}$, where n , n_e and n_p are the total, electron, and proton densities, respectively. Substituting the numerical values gives for the cooling time of the shocked

secondary’s wind

$$\tau_{\text{cool}2} = 1.1 \left(\frac{\dot{M}_2}{10^{-5} M_\odot \text{ yr}^{-1}} \right)^{-1} \left(\frac{D_{g2}}{0.2 \text{ AU}} \right)^2 \left(\frac{v_2}{3000 \text{ km s}^{-1}} \right)^{2.2} \text{ day}. \quad (17)$$

(Near periastron and for these parameters the post shock electron density is $\sim 10^{10} \text{ cm}^{-3}$ and the temperature $\sim 10^8 \text{ K}$; the equalization time of ion and electron temperature for these values is $\sim 0.1 \text{ day}$ (Usov 1002), shorter than the cooling time.) The fraction of the shocked wind that cools to very low temperatures and is compressed is (eq. 7 of Usov 1991) $\alpha \sim (\tau_{f2}/\tau_{\text{cool}2})^2$ which is ~ 0.01 near periastron passage. This implies that at periastron passage the shocked secondary’s wind within a distance of $\sim 0.1 D_{g2}$ from the stagnation point cools and is compressed. This will further reduce the support to the shocked primary’s wind against being accreted by the secondary.

2.3. Numerical Values

The parameters used in the present calculations are based on papers cited in previous sections (e.g., Pittard & Corcoran 2002; Martin et al. 2005). We take the primary’s wind to have a profile of $v_1 = 500[1 - (0.4 \text{ AU}/r_1)] \text{ km s}^{-1}$, where r_1 is the distance from the center of the primary; as this expression is a crude estimate of the acceleration zone of the primary’s wind, we can take $r_1 = r$ at the stagnation point. At periastron $r = 1.66 \text{ AU}$ and $v_1 = 380 \text{ km s}^{-1}$, larger than the speed assumed by Martin et al. (2005). Based on the results of Pittard & Corcoran (2002) the secondary’s wind speed is taken to be $v_2 = 3000 \text{ km s}^{-1}$, and the mass loss rates are assumed to be $\dot{M}_1 = 3 \times 10^{-4} M_\odot \text{ yr}^{-1}$ and $\dot{M}_2 = 10^{-5} M_\odot \text{ yr}^{-1}$. The masses are $M_1 = 120 M_\odot$ $M_2 = 30 M_\odot$ (Hillier et al. 2001), the eccentricity is $e = 0.9$ (Smith et al. 2004), and orbital period 2024 days, hence the semi-major axis is $a = 16.64 \text{ AU}$.

3. ACCRETION NEAR PERIASTRON PASSAGE

The relevant length scales and time scales derived in the previous section are plotted as function of the orbital phase, where phase zero is taken at periastron, in Figure 2. Note that phase zero corresponds to periastron passage. This is not to be confused with phase zero defined from observations of the intensities of different lines; in the latter cases phase zero is assumed to be near periastron, but may not correspond precisely to periastron passage (see footnote 4 in Martin et al. 2005).

Two ratios determine the importance of the secondary’s gravity: the accretion radius to stagnation distance $R_{\text{acc}2}/D_{g2}$, and the flow time of the shocked primary’s wind to the free fall time from the stagnation point $\tau_{\text{f}1}/\tau_{\text{ff}2}$. Over most of the orbital motion these ratios are very small (lower panel of Figure 2), and gravity is negligible. However, very close to periastron these ratios become ~ 0.5 . For example, both these ratios are larger than ~ 0.25 from 10 days before to 40 days after periastron passage. These large ratios suggest that accretion might take place near periastron passage. The asymmetry of these ratios around periastron fit well with the asymmetrical behavior of the event around periastron. For example, the X-ray emission after the flat minimum period does not return to its luminosity prior to the flat minimum period. This asymmetry results from the larger relative wind velocity $v_{\text{wind}1}$ as the system approaches periastron and $v_r < 0$, than when the system leaves periastron and $v_r > 0$ (eq. 1). This then influences the values of the stagnation distance (eq. 8) and the accretion radius (eq. 7), which determines the other properties, such as cooling time.

The exact flow structure requires 3D gas-dynamical simulations. However, we can suggest the following scenario already from the present results. Due to thermal instabilities (e.g., Stevens et al. 1992) dense large blobs are formed in the post-shock primary’s wind region near the stagnation point. These blobs are pulled to the secondary as periastron is approached. Very close, possibly ~ 10 day prior, to periastron passage the mass of the primary’s wind that is accreted is assumed to be large enough to shut down the secondary wind. The assumed shut-down must be non-linear because the mass accretion rate is smaller than the mass loss rate of the secondary. As the secondary’s wind no longer reaches the previous stagnation region, the entire primary’s wind entering the Bondi-Hoyle accretion cylinder, i.e. having an impact parameter smaller than the accretion radius, will be accreted by the secondary. In other words, the previously colliding winds region collapses onto the secondary. We emphasize that a key ingredient in the model is that blobs accreted near periastron passage shut down, or substantially weaken, the secondary wind, such that the accretion radius becomes larger than the stagnation distance. This allows more accretion that is *assumed* to shut down the secondary wind in several days. This process might occur even if during the time the first blobs are accreted the accretion radius is smaller than the stagnation distance.

In a steady state situation the mass accretion rate is $\dot{M}_{\text{acc}2} = \pi R_{\text{acc}2}^2 \rho_1 v_{\text{wind}1}$, which for the parameters used here reaches a maximum value of $\dot{M}_{\text{acc}2} \sim 0.006 \dot{M}_1 \simeq 10^{-6} M_{\odot} \text{ yr}^{-1}$. This is not a high accretion rate, compared with the mass blown by the secondary. However, a short time after the region near the stagnation point collapses this mass falls onto the secondary from one direction. As shown here and by Soker (2005) dense blobs can be accreted by the secondary. After the collapse of the stagnation point, the primary’s wind accelerates and its density increases as it approaches the secondary. It is assumed that the

accreted cold gas prevents the secondary’s normal wind acceleration. As the stars separate, the mass accretion rate then declines and the secondary wind reappear again, building the wind collision region, only when orbital separation increases again to several AU. The orbital separation is twice its periastron values (1.66 AU) after 20 days, and five times its periastron distance after 75 days. When the colliding winds region is built again, the X-rays reappear.

In a steady state accretion from a wind, the accreted mass possesses angular momentum. If the specific angular momentum is larger than that of a test particle performing Keplerian motion on the equator of the accreting star, an accretion disk might be formed. The condition for that is given by, e.g., Soker (2001a; eq. 1 there). Substituting the physical parameters used here, we find that in a steady state accretion the accreted primary’s wind possesses specific angular momentum which is too low by a factor of ~ 10 to form an accretion disk around the secondary. One of the reasons is that in the Bondi-Hoyle type accretion flow, the accretion flow rearranged itself to accrete a small fraction ($\sim 20\%$) of the angular momentum entering the Bondi-Hoyle accretion cylinder. However, during the brief collapse of the material near the stagnation point this reduction does not happen. Furthermore, the collision region near the stagnation point is larger than the accretion radius, and the specific angular momentum is larger. Over all, we suggest that an accretion disk does form for a brief period, a few days, during the collapse stage of the colliding wind region (the collapse of the stagnation point). Such an accretion disk could blow a collimated fast wind.

4. DISCUSSION AND SUMMARY

In the previous section we have shown that near periastron the secondary’s gravity becomes a significant factor in determining the flow near the stagnation point. Along most of the orbit the accretion radius ($R_{\text{acc}2}$; eq. 7), which characterized the influence of the secondary on the undisturbed primary wind, is much smaller than the distance of the stagnation point from the secondary (D_{g2} ; eq. 8). Along most of the orbit, the outflow time of the post-shock primary’s wind from the stagnation point vicinity ($\tau_{\text{f}1}$; eq. 16) is much shorter than the free fall time of this gas to the secondary ($\tau_{\text{ff}2}$; eq. 15). However, very close to periastron passage these two ratios, $R_{\text{acc}2}/D_{g2}$ and $\tau_{\text{f}1}/\tau_{\text{ff}2}$ (lower row of figure 2), increase to ~ 0.5 . This shows that the secondary significantly alters the flow such that it might accrete from the cool post-shock primary’s wind. We speculate that this could lead to the collapse of the wind collision region near the stagnation point. We further speculate that for a short time an accretion disk and a collimated fast wind might be formed. We note that the accretion phase is relatively short, and the steady state accretion rate relatively low ($\dot{M}_{\text{acc}2} \sim 10^{-6} M_{\odot} \text{ yr}^{-1}$; sec. 3). Therefore, the total accreted mass is negligible compared

with the mass lost in the secondary wind.

In addition to the assumptions made in developing the model, there are some not well determined binary parameters which introduce further uncertainties. We consider the results with regards to uncertainties in wind parameters quite robust. This is because the wind parameters are constrained by the X-ray properties (Pittard & Corcoran 2002). More than that, it is possible that the equatorial mass loss by the primary will increase near periastron passages (Pittard & Corcoran 2002; but see Soker 2005), hence enhancing accretion. The model is only slightly more sensitive to the eccentricity as long as $e \gtrsim 0.8$. If $e = 0.8$ instead of $e = 0.9$, for example, we find that the maximum ratio of $R_{\text{acc}2}/D_{g2}$ is 0.23 instead of 0.47 for $e = 0.9$. However, in the case $e = 0.9$ assumed in this paper, this ratio stays at a value of $R_{\text{acc}2}/D_{g2} > 0.2$ for ~ 65 days, about the length of the flat X-ray minimum. It is assumed here that for such a value the mass accretion rate is high enough to shut down the secondary wind. In the case of $e = 0.8$ the inequality $R_{\text{acc}2}/D_{g2} > 0.2$ holds for ~ 40 days, but the inequality $R_{\text{acc}2}/D_{g2} > 0.17$ holds for ~ 65 days. We see that the conditions for ~ 65 days accretion is not much different in the two cases. This suggests that even for $e = 0.8$ accretion might occur, and our model can hold even for eccentricity as low as $e = 0.8$. Of course, this depends on the validity of our assumptions that (i) accretion starts for these values of $R_{\text{acc}2}/D_{g2}$; and (ii) the accretion can shut down the secondary wind.

The suggestion of the collapse of the interacting winds region is disputed. Other researchers argue that the winds collision region (the stagnation point region) continues to exist during the X-ray minimum, e.g., Abraham et al. (2005) who based their claim on their suggestion that the 7 mm emission comes from this region.

In our proposed scenario the collapse of the wind collision region to the secondary is behind the long and almost flat minimum in the X-ray emission, lasting ~ 60 days (0.03 of the cycle) (Ishibashi et al. 1999; Corcoran et al. 2001a; Corcoran et al. 2004b; Corcoran 2005). The X-ray emission results from the collision of the two winds from the two stars (Corcoran et al. 2001a; Pittard & Corcoran 2002), as in similar massive binary systems (Usov 1992), most prominently, the WR-O binary system WR 140 (Williams et al. 1990). In the interacting massive binary system WR 140 the X-ray minimum is not flat, and it can easily be explained by absorption of the X-ray emission by the dense wind of the WR star (Corcoran et al. 2004b; Pollock et al. 2005). In η Car, the flat minimum in X-ray emission seems to be intrinsic (Corcoran et al. 2000; Hamaguchi et al. 2005), that is, a reduction in emission measure of the X-ray emitting gas, and the minimum is not easy to explain only by absorbing material. The hard ($\gtrsim 5\text{keV}$) X-ray emission drops by a factor of up to ~ 100 during the minimum, but there is still hard X-ray emission. In Akashi et al. (2006) this residual X-ray emission during minimum is explained in the frame of the accretion model.

After the collapse of the stagnation region, the primary’s wind collides with the secondary’s wind very close to the secondary, most likely within the acceleration zone of the secondary’s wind. In this type of wind interaction the secondary’s luminosity slows down the primary’s wind before it encounters the shock wave (Gayley et al. 1997), reducing substantially the X-ray intensity and making it softer (Usov 1992). The slowing down process by the secondary radiation pressure affects the location of the new stagnation point, but does not push it back to its original place. Hence, it cannot prevent the proposed collapse of the colliding wind region. In any case, this process is not relevant to η Car because the primary wind is too slow to contribute to the observed X-ray emission above 1keV. This is true even if the gravitational acceleration by the secondary is taken into account (Akashi et al. 2006). The effects of the secondary’s gravity and radiation on this asymmetrical flow are very complicated, and are postponed for discussion to a future paper. In addition to the reduction in the mass of the colliding primary’s wind and its deceleration, a substantial fraction of the X-rays emitted by the shocked winds is absorbed by the dense accreted mass (Akashi et al. 2006).

We also speculate that the accretion process is connected to the peak luminosity of the HeII λ 4687Å line. This peak occurs very shortly after the X-ray flux starts to decline (Steiner & Daminieli 2004; Martin et al. 2005). In a future paper we will examine the possibilities that the He line is emitted by the cooling secondary’s wind as its cooling time $\tau_{\text{cool}2}$ (eq. 17) becomes short (figure 2, row 2), or that the He line is emitted by a collimated outflow blown by the accreting secondary.

We thank an anonymous referee for detail and very helpful comments which substantially improved the presentation of the results. This research was supported in part by a grant from the Israel Science Foundation.

REFERENCES

- Abraham, Z., Falceta-Goncalves, D. Dominici, T. P., Nyman, L.-A., Durouchoux, P., McAuliffe, F., Caproni, A., & Jatenco-Pereira V. (astro-ph/0504180)
- Akashi, M., Soker, N., Behar, E. 2006, second paper in this series.
- Corcoran, M. F. 2005, AJ, 129, 2018
- Corcoran, M. F., Fredericks, A. C., Petre, R., Swank, J. H., & Drake, S. A. 2000, ApJ, 545, 420
- Corcoran, M. F., Hamaguchi, K., Gull, T., et al. 2004a, ApJ, 613, 381 (astro-ph/0406180)
- Corcoran, M. F., Ishibashi, K., Swank, J. H., & Petre, R., 2001a, ApJ, 547, 1034

- Corcoran, M. F., Pittard, J. M., Stevens, I. R., Henley, D. B., & Pollock, A. M. T. 2004b, in the Proceedings of "X-Ray and Radio Connections", Santa Fe, NM, 3-6 February, 2004 (astro-ph/0406294)
- Corcoran, M. F., Swank, J. H., Petre, R. et al. 2001b, *ApJ*, 562, 1031
- Damineli, A. 1996, *ApJ*, 460, L49
- Damineli, A., Conti, P. S., & Lopes, D. F. 1997, *NewA*, 2, 107
- Damineli, A., Kaufer, A., Wolf, B., Stahl, O., Lopes, D. F., & de Araujo, F. X. 2000, *ApJ*, 528, L101
- Danby, J. M. A.; Camm, G. L. 1957, *MNRAS*, 117, 50
- Davidson, K. Gull, T. R., Humphreys, R. M. et al. 1999, *AJ*, 118, 1777
- Davidson, K., & Humphreys, R. M. 1997, *ARA&A*, 35, 1
- Duncan, R. A., & White, S. M. 2003, *MNRAS*, 338, 425
- Fernandez Lajus, E., Gamen, R., Schwartz, M., Salerno, N., Llinares, C., Farina, C., Amorin, R., & Niemela, V. 2003 *Information Bulletin on Variable Stars*, 5477, 1 (astro-ph/0311437)
- Gayley, K. G., Owocki, S. P., & Cranmer, S. R. 1997, 475, 786
- Hamaguchi, K., Corcoran, M. F., Gull, T., White, N. E., Damineli, A., & Davidson, K. 2005 (astro-ph/0411271) proceeding of the workshop "Massive Stars in Interacting Binaries"
- Hillier, D. J., Davidson, K., Ishibashi, K., & Gull, T. 2001, *ApJ*, 553, 837
- Ishibashi, K., Corcoran, M. F., Davidson, K., Swank, J. H., Petre, R., Drake, S. A., Damineli, A., & White, S. 1999, *ApJ*, 524, 983
- Ishibashi, K., Gull, T., Davidson, K. et al. 2003, *AJ*, 125, 3222
- Martin, J. C., Davidson, K., Humphreys, R. M., Hillier, D. J., & Ishibashi K. 2005, *Astrophysical Journal*, (astro-ph/0504151)
- Martin, J. C., & Koppelman, M. D. 2004, *AJ*, 127, 2352 (astro-ph/0401254)
- Morse, J. A., Davidson, K., Bally, J., Ebbets, D., Balick, B., & Frank, A. 1998, *AJ*, 116, 2443
- Pittard, J. M., & Corcoran, M. F 2002, *A&A*, 383, 636
- Pollock, A. M. T., et al. 2005, *ApJ*, submitted
- Smith, N., Davidson, K., Gull, T.R., Ishibashi, K., & Hillier, D.J. 2003a, *ApJ*, 586, 432

- Smith, N., Gehrz, R., Hinz, P. M., Hoffmann, W. F., Hora, J.L., Mamajek, E. E., & Meyer, M. R. 2003b, *AJ*, 125, 1458
- Smith, N., Morse, J. A., Collins, N. R., & Gull, T. R. 2004, *ApJ*, 610, L105 (astro-ph/0406408)
- Soker, N. 2001a, *ApJ*, 558, 157
- Soker, N. 2001b, *MNRAS*, 325, 584
- Soker, N. 2003, *ApJ*, 597, 513
- Soker, N. 2004, *ApJ*, 612, 1060
- Soker, N. 2005, *ApJ*, 619, 1064
- Steiner, J. E., & Daminieli, A. 2004, *ApJ*, 612, L, 133
- Stevens, I. R., Blondin, J. M., & Pollock, A. M. T. 1992, *ApJ*, 386, 265
- Usov, V. V., 1991, *MNRAS*, 252, 49
- Usov, V. V., 1992, *ApJ*, 389, 635
- van Genderen, A. M., de Groot, M. J. H., & The, P. S. 1994, *A&A*, 283, 89
- van Genderen, A. M., Sterken, C., de Groot, A., & Burki, G. 1999 *A&A*, 343, 847
- van Genderen, A. M., Sterken, C., de Groot, A. et al. 1995 *A&A*, 304, 415
- Verner, E., Bruhweiler, F. & Gull, T. 2005 , *ApJ*, 624, 973 (astro-ph/0502106)
- Whitelock, P. A., Feast, M. W., Marang, F., & Breedt, E. 2004, *MNRAS*, 352, 447 (astro-ph/0404513)
- Williams, P. M., van der Hucht, K. A., Pollock, A. M. T., Florkowski, D. R., van der Woerd, H., & Wamsteker, W. M. 1990, *MNRAS*, 243, 662
- Zanella, R., Wolf, B., & Stahl, O. 1984, *A&A*, 137, 79

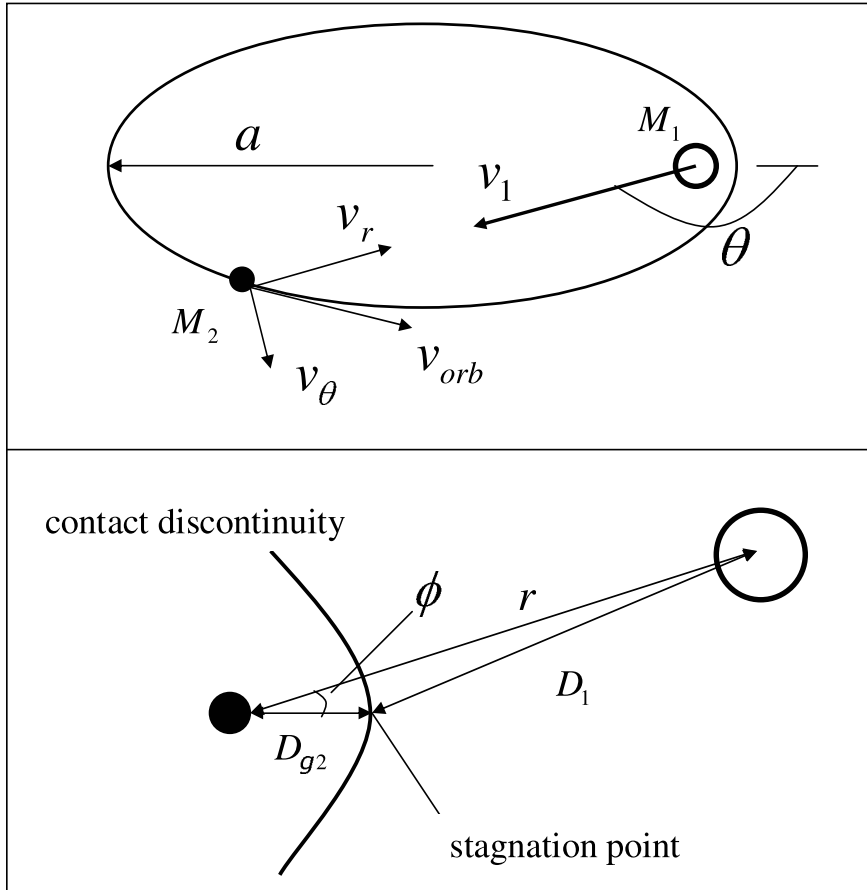


Fig. 1.— Upper panel: the orbit and relevant velocities in the rest frame of the primary star of mass M_1 . Drawn are the primary’s wind velocity v_1 , the two stars relative orbital velocity v_{orb} , and v_r and v_θ which are the radial and tangential components of v_{orb} , respectively. Lower panel: Geometrical definitions relevant to the flow near the stagnation point. The contact discontinuity is the surface where the two winds meet after they have passed the shock waves. The velocity directions in the lower panel are as in the upper panel (the secondary moves to the lower right.)

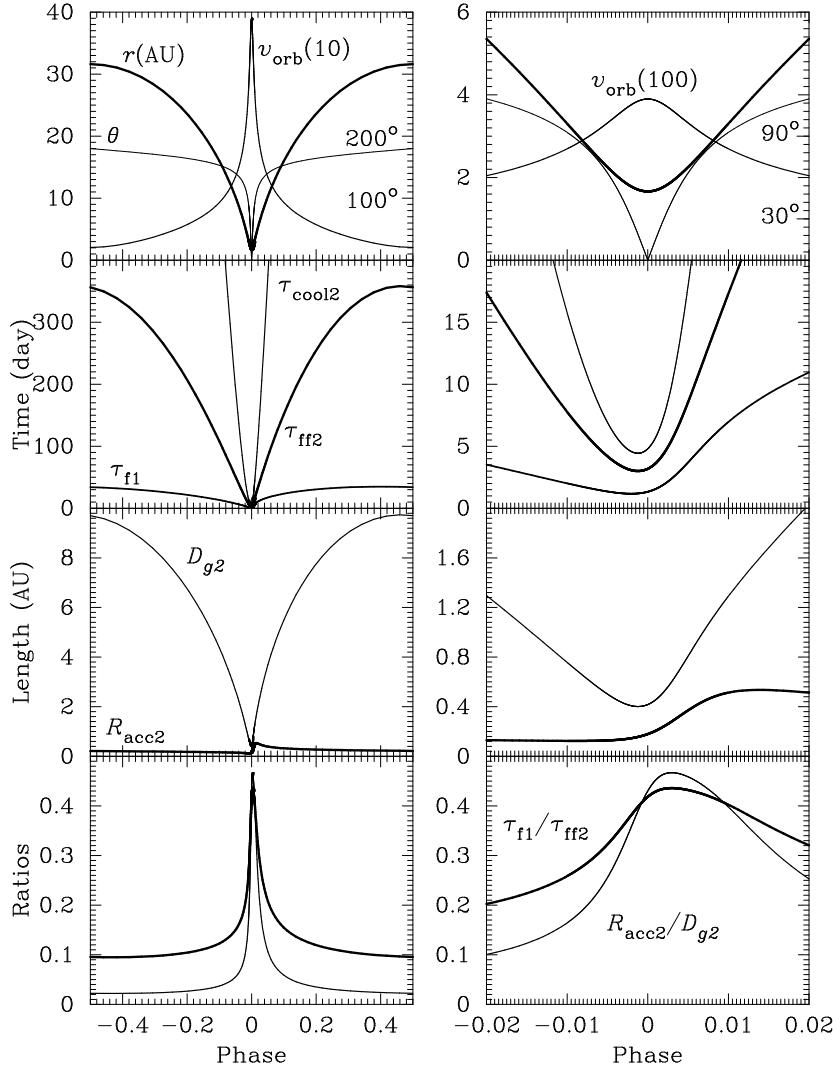


Fig. 2.— Several physical variables as function of orbital phase (phase zero is at periastron). The left column covers the entire orbit, while the column on the right covers the time just prior to and after periastron. Upper row: The orbital separation (in AU) and the relative orbital speed of the two stars (in 10 km s^{-1} on the left and 100 km s^{-1} on the right). The angle θ is the relative direction of the two stars as measured from periastron (scale on the right in degrees). Second row: The cooling time of the shocked secondary’s wind near the stagnation point (upper line; eq. 17), the free fall time from the stagnation point to the secondary (middle line; eq. 15), and the flow time of the primary wind from the stagnation point (lower line; eq. 16). Third row: the distance of the stagnation point from the secondary (upper line; eq. 8), and the Bondi-Hoyle accretion radius of the secondary star (lower line; eq. 7). Lower row: The ratio $R_{\text{acc}2}/D_{g2}$ (thin line) and $\tau_{\text{ff}1}/\tau_{\text{ff}2}$ (thick line).